

Glutathione- and Cysteine-Induced Transverse Overgrowth on Gold Nanorods

Xiaoshan Kou,[†] Shuzhuo Zhang,^{†,‡} Zhi Yang,[†] Chia-Kuang Tsung,[§] Galen D. Stucky,[§]
Lingdong Sun,[‡] Jianfang Wang,^{*,†} and Chunhua Yan[‡]

Department of Physics, Chinese University of Hong Kong, Shatin, Hong Kong, China, State Key Lab of Rare Earth Materials Chemistry and Applications, Peking University, Beijing 100871, China, and Department of Chemistry and Biochemistry, University of California, Santa Barbara, California 93106

Received February 13, 2007; E-mail: jfwang@phy.cuhk.edu.hk

Gold nanorods (NRs) exhibit strong optical extinction at their longitudinal plasmon wavelengths. They have been demonstrated to function as scattering¹ and two-photon chromophores² for bioimaging, biosensors,^{3,4} and agents for cancer therapy.⁵ They have also been incorporated into polymers and deposited onto bacteria to form optical and bioelectronic materials.⁶ Electrochemical,⁷ photochemical,⁸ and seed-mediated methods^{9–11} have been developed for growing Au NRs in cationic surfactant aqueous solutions. Major efforts have so far focused on the control of the lengths of NRs, for example, by the use of surfactants with different headgroups¹² and by means of multistep growth.^{9,10,12} Deliberate control of NR diameters has remained elusive.

Glutathione (GSH) is the most abundant thiol species in cells (intracellular 1–10 mM, extracellular <10 μM).¹³ It functions biologically in detoxification processes and protection against oxidant injury. Prior experiments have found that GSH can serve as triggers for drug release from Au nanoparticle carriers¹⁴ and as linkers for end-to-end assembly of Au NRs.^{4,15}

Here we report the transverse overgrowth on Au NRs induced by the binding of GSH or cysteine onto their ends (Figure 1). During overgrowth, Au NRs become wider and their lengths stay unchanged. Their shape undergoes a gradual change from rods, peanuts, and truncated octahedra to faceted spheres as the amount of the Au precursor is increased.

Original Au NRs were grown using the seed-mediated method in cetyltrimethylammonium bromide (CTAB) solutions in the presence of AgNO₃, as reported previously.^{11,12,16} Briefly, the seed solution was made by adding a freshly prepared, ice-cold NaBH₄ solution (0.3 mL, 0.01 M) into a mixture solution composed of HAuCl₄ (0.125 mL, 0.01 M) and CTAB (3.75 mL, 0.1 M). The NR growth solution was prepared by adding ascorbic acid (1.152 mL, 0.1 M) into a mixture solution composed of HAuCl₄ (7.2 mL, 0.01 M), AgNO₃ (1.08 mL, 0.01 M), and CTAB (171 mL, 0.1 M). This growth solution was used for both the preparation of the original Au NRs and transverse overgrowth. The original NRs were obtained by adding the seed solution (0.189 mL) into the growth solution (45.108 mL). For transverse overgrowth, a calculated volume of GSH (0.01 M) was first added into the as-grown original NR solution to obtain a GSH concentration of 100 μM. The resulting mixture solution was kept at room temperature for 2 h. Varying volumes of the growth solution were then added into aliquots of this mixture solution.

Figure 2A shows the extinction spectra (Hitachi U-3501 UV–visible/NIR spectrophotometer) of the growth products obtained by the addition of varying volumes of the growth solution into aliquots of the original Au NR solution containing 100 μM GSH. The original Au NRs have a longitudinal plasmon peak at 778 nm

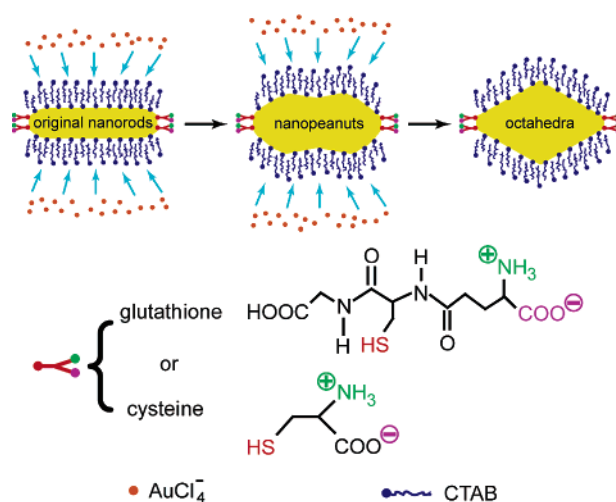


Figure 1. Schematic showing the transverse overgrowth on Au NRs induced by the selective binding of GSH or cysteine to their ends.

and a transverse one at 513 nm. As the volume of the growth solution is increased, the longitudinal plasmon peak gradually blue shifts and the transverse one slightly red shifts. They finally merge together at 559 nm. The complete growth of these products takes about 1 day [Supporting Information (SI) Figure S1]. The resulting samples exhibit distinct colors (SI Figure S2), with their longitudinal plasmon peak wavelengths tunable from ~560 nm to that of the original NRs. After complete growth, these NR samples are stable over a period of months without any observable shift in their longitudinal plasmon wavelengths. In contrast, the Au NRs grown by the seed-mediated method in one step in the presence of AgNO₃ are unstable, and their longitudinal plasmon peak can drift toward shorter wavelengths by as much as 100 nm over a period of hours to days.¹⁷

Transmission electron microscopy (TEM, FEI CM120) was used to characterize the size and shape evolution of the growth products (Figure 2B–G, SI Figure S3). The original NRs exhibit relatively narrow diameter and length distributions, and their ends are slightly wider than their middle sections (Figure 2B). After the addition of a small amount of the growth solution, the NRs grow wider, with the ends growing faster than the middle sections in the transverse direction (Figure 2C). As more of the growth solution is added, the growth products undergo a shape change from rods to peanuts (Figure 2D). With the supply of even more growth solution, the growth at the middle sections catches up with and eventually overtakes that at the ends (Figure 2E), and the shape of the products transforms from peanuts to truncated octahedra (Figure 2F). The increase in the growth rate at the middle sections relative to that at the ends is presumably due to the development of the

[†] Chinese University of Hong Kong.

[‡] Peking University.

[§] University of California, Santa Barbara.

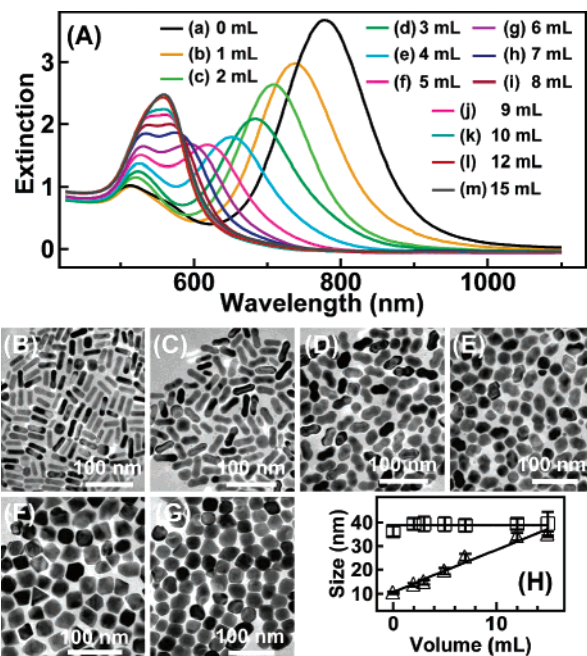


Figure 2. GSH-induced transverse overgrowth. (A) Extinction spectra of the growth products taken 1 day after the addition of varying volumes of the growth solution into 2.5 mL aliquots of the original Au NR solution containing 100 μM GSH. (B) TEM image of the original Au NRs. (C–G) TEM images of the products corresponding to the samples (c), (f), (h), (l), and (m) shown in (A), respectively. (H) Plots of the lengths (squares) and diameters (triangles) of the growth products as a function of the volume of the added growth solution. The lines are a guide to the eye. Size measurements were carried out on 200 particles per sample.

stable {111} facets of the face-centered cubic structure of gold. A further growth results in the formation of faceted Au spheres (Figure 2G).

The sizes of the growth products were measured from their TEM images. Since their thicknesses are not uniform along the length direction, the diameter at the middle was measured. The original Au NRs have an average diameter and length of 10.3 ± 0.9 and 36 ± 4 nm, respectively. During overgrowth, the length remains unchanged, indicating that the longitudinal growth is completely blocked. The diameter increases roughly linearly with the volume of the added growth solution (Figure 2H and SI Table S1). This leads to the reduction of the aspect ratio and the blue shift of the longitudinal plasmon peak (Figure 2A). The final production of faceted spheres causes the merging of the longitudinal and transverse plasmon peaks.

High-resolution (HR) TEM imaging (FEI Tecnai 20 ST) was further performed to characterize the crystal structures of the products obtained from the transverse overgrowth. Au NRs grown using the seed-mediated method in the presence of AgNO_3 have been shown to be single-crystalline with their side surfaces enclosed by the {100} and {110} facets.^{12,16} HRTEM imaging reveals that all of the growth products remain single-crystalline. Figure 3 shows representative lattice-resolved images of a peanut-like particle and a truncated octahedron. A majority of the growth products are oriented in the [110] direction under TEM imaging.

It has been suggested that Au NRs grown in CTAB solutions are encapsulated in a CTAB bilayer.¹⁸ Thiol molecules at low concentrations are preferentially bound to the ends of Au NRs, as demonstrated previously by the end-to-end assembly of Au NRs using various thiol molecules.^{4,15,19} This preferential binding is probably due to the fact that the CTAB bilayer is less ordered at the ends than that at the side surfaces of Au NRs. We therefore believe that the transverse growth with a complete blocking of the

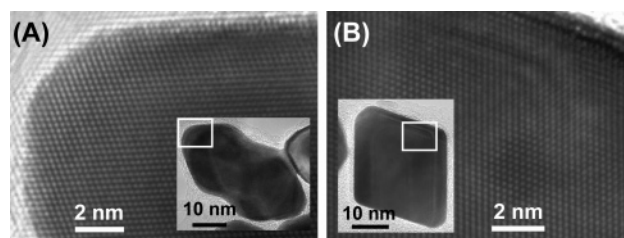


Figure 3. HRTEM images of (A) a nanopeanut and (B) an octahedron. The nanoparticles in (A) and (B) are from the samples (f) and (l) shown in Figure 2A, respectively. Both are oriented in the [110] direction.

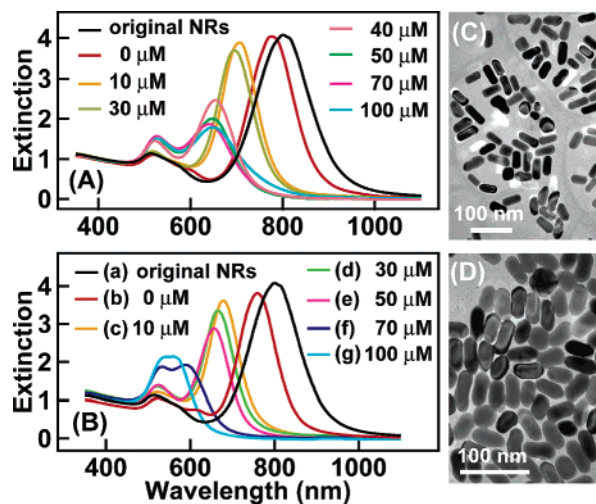


Figure 4. (A) Extinction spectra of the growth products obtained by the addition of 5 mL of the growth solution into 2.5 mL aliquots of the original Au NR solution that contains GSH at varying concentrations. (B) Extinction spectra of the growth products obtained by the addition of 10 mL of the growth solution into 2.5 mL aliquots of the original Au NR solution that contains GSH at varying concentrations. (C and D) TEM images of the growth products corresponding to the samples (c) and (e) shown in (B), respectively.

longitudinal growth is induced by the preferential binding of GSH to the ends of Au NRs (Figure 1).

Many control experiments were carried out to understand and verify this transverse overgrowth. First, the overgrowth was performed at varying GSH concentrations. The NR concentration in the as-grown solution is estimated to be ~ 1 nM according to previously measured extinction coefficients at the longitudinal plasmon wavelength.²⁰ It was found that there exists an optimal GSH concentration of ~ 100 μM for inducing the transverse growth while completely blocking the longitudinal growth. Figure 4A and B shows the extinction spectra of the products grown at varying GSH concentrations up to 100 μM by the use of 5 and 10 mL of the growth solution, respectively. It is observed that the products obtained at GSH concentrations lower than 100 μM have longer longitudinal plasmon wavelengths and therefore larger aspect ratios than those obtained at 100 μM GSH. This suggests that the average lengths of the products obtained at lower GSH concentrations are larger than those obtained at 100 μM GSH if the amount of the consumed Au precursor is assumed to be equal. Therefore, the longitudinal growth is not completely blocked at lower GSH concentrations. This incomplete blocking is further confirmed by TEM imaging. The products obtained at lower GSH concentrations are larger in both diameter and length than the original NRs (Figure 4C,D, and SI Table S1). In addition, a considerable percentage of the products exhibit one fat end, suggesting that the longitudinal growth is partially blocked. At GSH concentrations higher than 100 μM , Au NRs are linearly assembled, and both the transverse

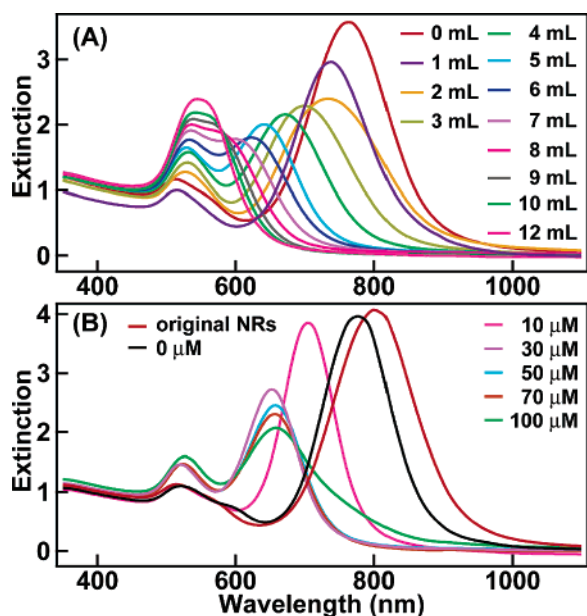


Figure 5. (A) Extinction spectra of the growth products obtained by the addition of varying volumes of the growth solution into 2.5 mL aliquots of the original Au NR solution containing 100 μM cysteine. (B) Extinction spectra of the growth products obtained by the addition of 5 mL of the growth solution into 2.5 mL aliquots of the original Au NR solution that contains cysteine at varying concentrations.

and longitudinal growth are blocked, as revealed by the extinction spectra (SI Figure S4).

Second, the overgrowth experiment performed in the presence of cysteine shows that cysteine can also induce the transverse overgrowth and that the optimal cysteine concentration for a complete blocking of the longitudinal growth is also $\sim 100 \mu\text{M}$ (Figure 5 and SI Figure S5). On the other hand, the sole transverse overgrowth was not observed for 3-mercaptopropionic acid (MPA) (SI Figure S6) or 11-mercaptoundecanoic acid (MUA) (SI Figures S7 and S8), although they also contain a thiol group. Cysteine and GSH contain both carboxyl and amino groups. They are present in the zwitterionic form in the Au NR solutions with a pH of ~ 4 . MPA and MUA possess only carboxyl groups. Our experimental results suggest that the blocking of the longitudinal growth over Au NRs is probably induced by the bound GSH and cysteine molecules through their zwitterionic groups. It has been reported that heat treatment can also yield fatter Au NRs by reducing unreacted Au precursor.²¹ However, the CTAB bilayer is probably destroyed at higher temperatures and a reshaping process is involved. This is different from our GSH- and cysteine-induced transverse overgrowth at room temperature.

Third, the overgrowth carried out without the use of thiol molecules indicates that both the diameters and lengths of the obtained NRs increase considerably with the volume of the growth solution (SI Figures S9 and S10, and Table S1). This is consistent with previous experiments on the overgrowth of Au, Ag, and Pt on Au NRs, where both the average lengths and diameters of the resulting products have been found to be larger than those of the original Au NRs, irrespective of the type of the metal precursor used in the second growth step.^{10,12,22,23}

In summary, we have demonstrated GSH- and cysteine-induced transverse overgrowth on Au NRs. GSH and cysteine are prefer-

entially bound to the ends of Au NRs, which blocks their longitudinal growth completely. As a result, the diameters of Au NRs become larger and larger while their lengths remain unchanged, as more and more growth solution is supplied. This transverse overgrowth provides an alternative means for tailoring both the longitudinal plasmon wavelengths and extinction cross sections of Au nanoparticles and will therefore facilitate their use in optics, optoelectronics, and biotechnology.

Acknowledgment. This work was supported by the RGC Direct Allocation through CUHK under the Project Code of 2060285 and a RGC grant under the Project Code of 2160293.

Supporting Information Available: Extinction spectra and TEM images of the products grown in the presence of different thiol molecules. This material is available free of charge via the Internet at <http://pubs.acs.org>.

References

- (1) Sönnichsen, C.; Alivisatos, A. P. *Nano Lett.* **2005**, *5*, 301.
- (2) (a) Bouhelier, A.; Bachelot, R.; Lerondel, G.; Kostcheev, S.; Royer, P.; Wiederrecht, G. P. *Phys. Rev. Lett.* **2005**, *95*, 267405. (b) Wang, H. F.; Huff, T. B.; Zweifel, D. A.; He, W.; Low, P. S.; Wei, A.; Cheng, J.-X. *Proc. Natl. Acad. Sci. U.S.A.* **2005**, *102*, 15752.
- (3) Li, C.-Z.; Male, K. B.; Hrapovic, S.; Luong, J. H. T. *Chem. Commun.* **2005**, 3924.
- (4) Sudeep, P. K.; Joseph, S. T. S.; Thomas, K. G. *J. Am. Chem. Soc.* **2005**, *127*, 6516.
- (5) Huang, X. H.; El-Sayed, I. H.; Qian, W.; El-Sayed, M. A. *J. Am. Chem. Soc.* **2006**, *128*, 2115.
- (6) (a) Pérez-Juste, J.; Rodríguez-González, B.; Mulvaney, P.; Liz-Marzán, L. M. *Adv. Funct. Mater.* **2005**, *15*, 1065. (b) Murphy, C. J.; Orendorff, C. J. *Adv. Mater.* **2005**, *17*, 2173. (c) Berry, V.; Gole, A.; Kundu, S.; Murphy, C. J.; Saraf, R. F. *J. Am. Chem. Soc.* **2005**, *127*, 17600.
- (7) Yu, Y.-Y.; Chang, S.-S.; Lee, C.-L.; Wang, C. R. C. *J. Phys. Chem. B* **1997**, *101*, 6661.
- (8) Kim, F.; Song, J. H.; Yang, P. D. *J. Am. Chem. Soc.* **2002**, *124*, 14316.
- (9) (a) Jana, N. R.; Gearheart, L.; Murphy, C. J. *J. Phys. Chem. B* **2001**, *105*, 4065. (b) Busbee, B. D.; Obare, S. O.; Murphy, C. J. *Adv. Mater.* **2003**, *15*, 414. (c) Wu, H.-Y.; Chu, H.-C.; Kuo, T.-J.; Kuo, C.-L.; Huang, M. H. *Chem. Mater.* **2005**, *17*, 6447.
- (10) Nikoobakht, B.; El-Sayed, M. A. *Chem. Mater.* **2003**, *15*, 1957.
- (11) Sau, T. K.; Murphy, C. J. *Langmuir* **2004**, *20*, 6414.
- (12) (a) Kou, X. S.; Zhang, S. Z.; Tsung, C.-K.; Yeung, M. H.; Shi, Q. H.; Stucky, G. D.; Sun, L. D.; Wang, J. F.; Yan, C. H. *J. Phys. Chem. B* **2006**, *110*, 16377. (b) Kou, X. S.; Zhang, S. Z.; Tsung, C.-K.; Yang, Z.; Yeung, M. H.; Stucky, G. D.; Sun, L. D.; Wang, J. F.; Yan, C. H. *Chem.—Eur. J.* **2007**, *13*, 2929.
- (13) (a) Smith, C. V.; Jones, D. P.; Guenther, T. M.; Lash, L. H.; Lauterburg, B. H. *Toxicol. Appl. Pharmacol.* **1996**, *140*, 1. (b) Schafer, F. Q.; Buettner, G. R. *Free Radical Biol. Med.* **2001**, *30*, 1191.
- (14) (a) Verma, A.; Simard, J. M.; Worrall, J. W. E.; Rotello, V. M. *J. Am. Chem. Soc.* **2004**, *126*, 13987. (b) Hong, R.; Han, G.; Fernández, J. M.; Kim, B.-J.; Forbes, N. S.; Rotello, V. M. *J. Am. Chem. Soc.* **2006**, *128*, 1078.
- (15) Zhang, S. Z.; Kou, X. S.; Yang, Z.; Shi, Q. H.; Stucky, G. D.; Sun, L. D.; Wang, J. F.; Yan, C. H. *Chem. Commun.* **2007**, DOI:10.1039/B618818D.
- (16) Tsung, C.-K.; Kou, X. S.; Shi, Q. H.; Zhang, J. P.; Yeung, M. H.; Wang, J. F.; Stucky, G. D. *J. Am. Chem. Soc.* **2006**, *128*, 5352.
- (17) Zweifel, D. A.; Wei, A. *Chem. Mater.* **2005**, *17*, 4256.
- (18) Nikoobakht, B.; El-Sayed, M. A. *Langmuir* **2001**, *17*, 6368.
- (19) (a) Caswell, K. K.; Wilson, J. N.; Bunz, U. H. F.; Murphy, C. J. *J. Am. Chem. Soc.* **2003**, *125*, 13914. (b) Thomas, K. G.; Barazzouk, S.; Ipe, B. I.; Joseph, S. T. S.; Kamat, P. V. *J. Phys. Chem. B* **2004**, *108*, 13066. (c) Chang, J.-Y.; Wu, H. M.; Chen, H.; Ling, Y.-C.; Tan, W. H. *Chem. Commun.* **2005**, 1092.
- (20) (a) Liao, H. W.; Hafner, J. H. *Chem. Mater.* **2005**, *17*, 4636. (b) Orendorff, C. J.; Murphy, C. J. *J. Phys. Chem. B* **2006**, *110*, 3990.
- (21) Gou, L. F.; Murphy, C. J. *Chem. Mater.* **2005**, *17*, 3668.
- (22) (a) Liu, M. Z.; Guyot-Sionnest, P. *J. Phys. Chem. B* **2004**, *108*, 5882. (b) Song, J. H.; Kim, F.; Kim, D.; Yang, P. D. *Chem.—Eur. J.* **2005**, *11*, 910.
- (23) (a) Grzelczak, M.; Pérez-Juste, J.; Rodríguez-González, B.; Liz-Marzán, L. M. *J. Mater. Chem.* **2006**, *16*, 3946. (b) Xiang, Y. J.; Wu, X. C.; Liu, D. F.; Jiang, X. Y.; Chu, W. G.; Li, Z. Y.; Ma, Y.; Zhou, W. Y.; Xie, S. S. *Nano Lett.* **2006**, *6*, 2290.

JA0710508